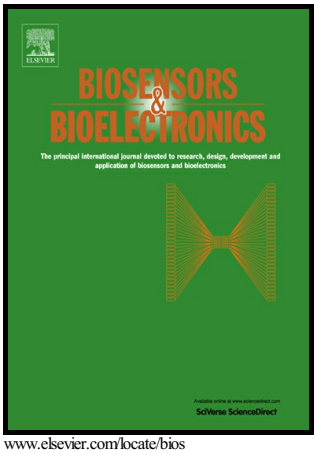

www.elsevier.com/locate/bios

Regenerative biosensor for use with biotinylated bait molecules

Claudia Knoglinger, Andreas Zich, Lukas Traxler, Kristyna Posledni, Gloria Friedl, Bianca Ruttmann, Anika Schorpp, Katharina Müller, Mirjam Zimmermann, Hermann J. Gruber

PII: S0956-5663(17)30482-7
DOI: http://dx.doi.org/10.1016/j.bios.2017.07.033
Reference: BIOS9866

To appear in: *Biosensors and Bioelectronic*

Received date: 26 April 2017
Revised date: 10 July 2017
Accepted date: 12 July 2017

Cite this article as: Claudia Knoglinger, Andreas Zich, Lukas Traxler, Kristyna Posledni, Gloria Friedl, Bianca Ruttmann, Anika Schorpp, Katharina Müller Mirjam Zimmermann and Hermann J. Gruber, Regenerative biosensor for us with biotinylated bait molecules, *Biosensors and Bioelectronic* http://dx.doi.org/10.1016/j.bios.2017.07.033

Regenerative biosensor for use with biotinylated bait molecules

Claudia Knoglinger, Andreas Zich, Lukas Traxler, Kristyna Posledni, Gloria Friedl, Bianca Ruttmann, Anika Schorpp, Katharina Müller, Mirjam Zimmermann, Hermann J. Gruber*

Institute of Biophysics, Johannes Kepler University Linz, Gruberstrasse 40, 4020 Linz, Austria

*Corresponding author. Tel.: +43 (732) 2468-7597. hermann.gruber@jku.at (H. J. Gruber)

ABSTRACT:

Label-free biosensors are ideally suited for the quantitative analysis of specific interactions among biomolecules or of biomolecules with drugs, as well as for quantitation of diagnostic markers in biofluids. In contrast to the label-dependent methods, a new assay for a particular prey molecule can be set up within few minutes by immobilizing the corresponding bait molecule on the sensor surface, using one of the common immobilization procedures. Unfortunately, the extensive application of label-free biosensors is still hampered by the fact that the immobilization of the bait molecule is usually irreversible; for that reason, a new chip (which is expensive) is required for every successful or futile attempt. Here, we present a general method for the switchable immobilization of biotinylated bait molecules on a new desthiobiotin surface, using wild-type streptavidin as a robust bridge between the chip and the biotinylated bait. The immobilization of the bait is very stable, so that many cycles of prey injection and subsequent prey removal can be carried out. For the latter, common reagents like HCl, Na_2CO_3, glycine buffer, or SDS are employed. When desired, however, streptavidin plus the biotinylated bait can be completely removed by 3 min injections of biotin, guanidinium thiocyanate, pepsin, and SDS, which makes it possible to immobilize new biotinylated bait. The number of *in situ* regeneration cycles is unlimited during the lifetime of the chip (2-3 weeks). One chip can easily be shared by many users with unrelated tasks (as is typical in academics), or used for the fully automated screening of many different interactions (for example in pharmaceutical research). In comparison to other regenerative chips, the new chip surface has much wider applicability and all of its structural and functional parameters have been disclosed.

Keywords: Regenerative biosensor, Desthiobiotin surface, Wild-type streptavidin, Reversible immobilization, Surface plasmon resonance

1. Introduction

Label-free biosensors are ideally suited for studying the kinetics and equilibria of reversible interactions between biomolecules. Thereby, one of the interacting components (the "bait") is immobilized on the sensor surface and binding/dissociation of the complementary soluble component (the "prey") is monitored in real time [Cooper, 2009]. Unfortunately, the widespread use of biospecific interaction analysis (BIA) is hampered by several factors: (i) The cost per sensor chip is high. (ii) Immobilization of the bait on the chip is usually irreversible, and therefore each successful or futile test with a new bait requires a new chip. (iii) Many immobilization protocols are not invariant but have to be adapted for different baits by trial and error.

Immobilization of biotinylated bait molecules on streptavidin chips is simpler than covalent coupling, but the immobilization is essentially irreversible [Green, 1990]. The latter limitation was overcome by two strategies which allow for switchable immobilization and removal of (strept)avidin. In the Biotin CAPture Kit™ (GE Healthcare product No. 28920233), both streptavidin and the dextran chip surface are derivatized with complementary oligonucleotides and immobilization is achieved by hybridization. The resulting double helix is stable for as long as needed but can be dissociated by a pulse of 100 mM HCl, which results in the complete regeneration of the chip surface. This chip cannot be used for DNA-binding proteins; its capacity is not higher than that of two-dimensional surfaces, and it is only available for one brand of biosensor.

In the second strategy, a biotin-avidin-biotin bridge is formed between a biotinylated self-assembled monolayer (SAM) and the biotinylated bait molecules, as depicted in Scheme 1A [Pollheimer et al., 2013; Taskinen et al., 2014; Zauner et al., 2016]. The high stability of the bridge allows for repeated binding and dissociation of prey molecules (states 3 and 4 in Scheme 1A). When desired, however, avidin with the mutation M96H can be dissociated into non-functional monomers (state 5b) by a combination of SDS and citric acid; this results in the full regeneration of the biotin surface. The undesired non-specific adsorption of nucleic acids to avidin was eliminated by additional mutations which lowered the *pI* from 10.5 to 7.0 [Taskinen et al., 2014]. When that was done, however, the biotin-avidin-biotin bridge was no longer perfectly stable under conditions typically used for prey removal [Zauner et al., 2016]. Unfortunately, this kind of avidin mutant had serious disadvantages; the high stability of avidin M96H was associated with high non-specific adsorption, whereas multiply mutated avidin, which had a low non-specific adsorption, was not sufficiently stable, and therefore could not be used for routine application in biosensing.

The goal of the present study was to find a solution which simultaneously provides for (i) low non-specific adsorption, (ii) high stability of the biotin-avidin-biotin bridge under typical working conditions, and (iii) complete rupture of the biotin-avidin-biotin bridge when this was desired. This goal was achieved by using *wild-type* streptavidin in place of the avidin mutants (see Scheme 1A). The advantages of streptavidin are its low *pI*, its low non-specific adsorption of DNA and protein, and its robustness under a wide range of buffer conditions [Green, 1990]. The major difficulty was in finding a method for switching off the robust bond between streptavidin and the biotin chip. Initial attempts on the biotin-SAM of Pollheimer et al. [2013] were unsuccessful, even when extreme denaturants were used (see section S8 in the Supplementary Information). The replacement of biotin by iminobiotin was not an option because the affinity of that latter substance for streptavidin is too weak [Raphael et al., 2011]. Although desthiobiotin initially appeared more promising, in all published examples [Knoll et al., 2000; Yoon et al., 2001; Hirsch et al., 2002] the dissociation of streptavidin from desthiobiotin surfaces was rather incomplete, even after hours of washing with biotin-containing buffer.

The aforementioned desthiobiotin surfaces are unfavorable for biosensing because they are not protein-resistant. PAMAM particles as used by Yoon et al. [2001] are known to cause non-specific adsorption of proteins [Matsumoto et al., 2011]. The same applies to the desthiobiotin-SAM used by Knoll et al. [2000] which is depicted in Fig. 1A. Ninety percent of this SAM consisted of mercaptoundecanol (**1**), which strongly adsorbs proteins [Prime et al., 1991].

In a recent study, we replaced the desthiobiotin-SAM of Fig. 1A with the new desthiobiotin-SAM shown in Fig. 1B. It exhibits the same high protein resistance as the analogous biotin-SAM and allows for complete regeneration according to Scheme 1A [Gruber, 2017]. As shown below in much greater detail, this strategy enabled us to accomplish all of our desired goals: (i) very low non-specific adsorption of protein and nucleic acids, (ii) stable binding of streptavidin and biotinylated baits for as long as was desired, and (iii) complete removal of streptavidin and biotinylated baits in a matter of minutes when a novel washing protocol was employed.

2. Materials and Methods

2.1. Materials

The matrix alkanethiol derivative (MAT, **3**) was synthesized as described [Pollheimer et al., 2013]. The desthiobiotin alkanethiol derivative (DBAT, **4**) was synthesized and mixed with MAT under reducing conditions, as described in the Supplementary Information (Charts S1 and S2, respectively). Most of the buffers, proteins, and nucleic acids were the same as the ones used in the previous studies with switchable avidin mutants [Zauner et al., 2016]. A detailed description of their preparation is given in the Supplementary Information (section S3). The same also applies to the additional components used in Section 3.7.

Biotin (200 mM, pH 8-8.5) was prepared by dissolving 1 mmol biotin and 1.3 mmol Tris base in water in a final volume of 5 ml and then, if needed, correcting the pH (according to pH paper) by further addition of Tris base. It was divided into single-use aliquots and stored at -25°C. Guanidinium thiocyanate (GTC, 6 M) was prepared by dissolving 7.09 g GTC in 4.28 ml water and stored at room temperature, whereby exposure to light was avoided (CAUTION: GTC must not be mixed with acid because this will result in the release of toxic HSCN gas!). Pepsin (2 mg/ml) was dissolved in 1 M glycine (pH 2.5 adjusted with HCl) and stored for 2 weeks at 4°C. SDS (0.5%) was dissolved in water and kept at room temperature.

2.2. Surface plasmon resonance experiments.

Cleaning of the bare glass chips, evaporation of the chromium (3 nm) and the gold (41 nm), as well as the cleaning of the gold surface and the coating with the mixed SAM was performed as described [Pollheimer et al., 2013], except that the biotin alkanethiol derivative (BAT, Chart S4) was replaced by DBAT (Fig. 1B). Details are found in the Supplementary Information (Section S2). The chips were mounted on the chip supports with double-sided adhesive tape (non-permanent) and inserted into a BIAcore X® device for measurement of binding by surface plasmon resonance (SPR). Filtered (0.45 µm) and degassed buffer was run over the chip surface, typically at 20 µl/min, as stated in the figure legends. The resonance angle was recorded at 1 s intervals and expressed in resonance units (1 RU = 0.0001°).

In most experiments the desthiobiotin chip was first covered with a monolayer of streptavidin (injected at 2 µM concentration for 3 min) in both flow cells. Then, a biotinylated bait or biotinylated bovine serum albumin (biotin-BSA) was separately applied to flow cell 1 (FC1) or flow cell 2 (FC2), as specified in the figures. The prey molecules were injected in both flow cells, whereby the sample buffer and the running buffer usually contained a low

concentration of BSA, as is stated. All experiments were terminated by complete chip regeneration, typically by sequential injections of free biotin, guanidinium thiocyanate (GTC), pepsin, and SDS, as is specified.

3. Results and discussion

3.1. Reversible immobilization of streptavidin on the mixed desthiobiotin-SAM

The new desthiobiotin component (DBAT, **4**) was synthesized, mixed with a 4-fold molar amount of matrix component (MAT, **3**) under reducing conditions (Chart S2), and used to prepare the mixed SAM depicted in Fig. 1B. The binding capacity for streptavidin was high (2340 ± 70 RU, Fig. 1C). Initially, we tried to remove bound streptavidin with guanidinium chloride (6 M), or HCl (100 mM), or with a combination thereof, but most of the streptavidin remained bound (data not shown). Guanidinium thiocyanate, however, caused complete removal within a few seconds, as can be seen from the initial spike of each GTC injection (Fig. 1C). Binding and desorption of streptavidin could be repeated with perfect reproducibility, as demonstrated in Fig. 1C.

3.2. Reversible immobilization of biotinylated bait molecules

GTC was able to remove a streptavidin monolayer (Fig. 1C and red trace in Fig. 1D) but not the double layer formed between biotinylated IgG and streptavidin (blue trace in Fig. 1D). Fortunately, complete removal of all the protein molecules was achieved during the subsequent 3 min injection of pepsin (blue trace in Fig. 1D). As a consequence, the chip could repeatedly be functionalized with streptavidin and biotinylated IgG, whereby the extent of protein immobilization was fully reproducible (Fig. 1C).

The need for pepsin is explained by the illustration in Scheme 1B. At the given desthiobiotin density (20 mol-%) on the chip, streptavidin binds two desthiobiotin groups, while the two remaining binding sites are available for biotinylated baits [Jung et al., 2000]. At the same time, the biotinylated IgG carries several biotin labels per protein. Consequently, a continuous network is formed by the two proteins on the chip surface; it can only be dissolved by digestion with a protease. This behavior was not only observed with biotin-IgG (Figs. S1-S2, see Supplementary Information) but also with biotin-BSA (Fig. S3) and biotin-protein G (Fig. S5). In contrast, no pepsin was required for the removal of mono-biotinylated BSA (Fig. S4), because no crosslinking is possible if the bait carries a single biotin residue (see Scheme 1C). Together, these findings indicate (i) that GTC is only able to dissociate desthiobiotin but not biotin groups from the streptavidin molecules, and (ii) that the streptavidin tetramers are not dissociated by 6 M GTC (Scheme 1A, state 5a). Avidin M96H (state 5b), in contrast, is dissociated into monomers by SDS/citric acid [Pollheimer et al., 2013].

Figs. S1 and S2 show that the order in which pepsin and GTC are injected is not critical. Nevertheless, we decided to always apply GTC before pepsin for two reasons: (i) It makes sense to first denature the protein by GTC, which makes it more vulnerable to the protease. (ii) In the optimized protocol (Fig. 2), the initial biotin injection must be followed by GTC (see chapter S7), so that pepsin and SDS serve as backups for the removal of the last remnants.

Admittedly, GTC was able to remove a fraction of biotin-IgG when it was mixed with tris(2-carboxyethyl)phosphine (TCEP, see blue trace in Fig. 1D). The combination of GTC and TCEP was much more effective than either reagent alone (Fig. S1), yet even repeated injections never achieved complete removal of the biotin-IgG and the streptavidin (Fig. S1). In the end, TCEP was eliminated from the list of regeneration reagents for the following

reasons: (i) TCEP can only enhance the decomposition of proteins like IgG, where multiple subunits are connected via disulfide bridges. (ii) The GTC, the base and the acidic TCEP hydrochloride must be mixed immediately before the injection, which is inconvenient and cannot be done in standard autosamplers. (iii) The addition of acidic TCEP to GTC before the base will result in the release of toxic HSCN gas. (iv) Two cycles of the TCEP-free injection series "GTC, pepsin, and SDS" were found to achieve complete chip regeneration, even in difficult cases (see Fig. S5).

The cycles shown in Figs. 1C and 1D could be repeated as often as desired, but after 2-3 weeks the binding capacity started to decrease. Before the weekend, the chip was washed inside the biosensor with water and then transferred into an argon filled Falcon™ tube with the cassette, where it was stored at 4°C.

3.3. The roles of free biotin, GTC, pepsin, and SDS in rapid chip regeneration

As mentioned in the introduction, several studies described the use of free biotin for removal of (strept)avidin from desthiobiotin surfaces [Knoll et al., 2000; Yoon et al., 2001; Hirsch et al., 2002] but the extent of removal was always well below 100%, even after extensive washing with free biotin at concentrations ranging from 0.1 to 50 mM. Chip regeneration protocols are only useful if the complete regeneration occurs within a few minutes. For this reason, we tested whether much higher concentrations of free biotin can remove streptavidin and biotinylated proteins from the desthiobiotin chip on this short time scale. Indeed, almost complete removal of streptavidin and biotin-BSA occurred during a 3-min injection of 200 mM biotin at pH 8 (Fig. 2), and the minor remnants were removed by a 3-min injection of GTC. In Fig. 2, the subsequent injections of pepsin and SDS appeared unnecessary but later it turned out that this is not generally true (see Fig. 3B). The only protocol which never failed was the sequence "biotin, GTC, pepsin, and SDS", and therefore it was adopted as the standard regeneration protocol.

Biotin concentrations above 200 mM (or longer washing with 200 mM biotin than for 3 min) turned out to be counterproductive, because free biotin progressively binds to the SAM with progressive tightness (Figs. S8-S10). The adsorption of free biotin was fully reversed by 6 M GTC, but only if ≤200 mM biotin was injected for ≤3 min (as in Fig. 2), and not after more extensive application of free biotin (Figs. S8-S10).

The dramatic effect of 200 mM biotin in Fig. 2 indicates that this high biotin concentration is able to dissociate not only the desthiobiotin-streptavidin bonds but also the biotin-streptavidin bonds which form the network depicted in Scheme 1B. It came as a great surprise that 200 mM biotin can do this, while 6 M GTC cannot (see Fig. 1D). We therefore examined whether 200 mM biotin (pH 8) acts by a double mechanism: (i) specific competition for biotin-binding sites and (ii) general destabilization of protein folding.

The latter aspect was tested by measuring the melting transition (T_m) of myoglobin in 100-500 mM biotin (pH 8) and parallel comparison with the effect of different urea concentrations (Figs. S7-S8). In these experiments, 200 mM biotin had the same effect as 1.5 M urea (ΔT_m = -5°C), and 500 mM biotin was equi-effective with 3 M urea (ΔT_m = -12°C). The data indicate that free biotin is a strong denaturant when used at high concentration. These findings can be explained by the structural features of biotin: (i) At pH 8, biotin has a detergent-like structure, with a long hydrophobic chain and a carboxylate anion. (ii) Thioether structures are known to undergo enhanced interaction with proteins, as exploited in thiophilic adsorption chromatography [Porath et al., 1985]. (iii) The ureido structure of biotin resembles urea, which is known for its denaturation potency. At 200 mM biotin, the synergy between the three structural aspects appears to cause a general destabilization of streptavidin, leading to the accelerated replacement of desthiobiotin and the biotinylated bait by free biotin.

The efficient dissociation of biotinylated baits from streptavidin by 200 mM biotin nourished hopes that high concentrations of free biotin might be able to remove streptavidin from the analogous *biotin*-SAM (Chart S4). Unfortunately, this idea turned out to be wrong. Although free biotin was much less effective than GTC and pepsin on the regular biotin-SAM, the latter reagents were also unable to remove all of the proteins from the biotin-SAM (Figs. S11-S12).

In conclusion, only the desthiobiotin-SAM (and not the analogous biotin-SAM) turned out to be fully regenerative, and the regeneration protocol in Fig. 2 was found to be superior to all of the alternatives concerning reagent concentrations and injection times.

3.4. Low non-specific adsorption of protein and nucleic acids

Fig. 3A reveals that the desthiobiotin-SAM depicted in Fig. 1B meets an essential criterion for practical application in biosensing: low non-specific adsorption of protein, both before and after the binding of streptavidin. The first injection with SDS caused no positive or negative change of the baseline, which means that SDS did not bind and that nothing had been adsorbed on the chip before this injection. Injection of a high BSA concentration showed only a transient bulk effect but also did not result in binding. The same was true for the injection of biotin-blocked streptavidin in flow cell 1 (FC1, see red text in Fig. 3A). Unblocked streptavidin, however, was bound with high efficiency in both flow cells (2430 and 2390 RU in FC1 and FC2, respectively). Subsequently, lysozyme and BSA (2×) were injected at high concentrations (1 mg/ml), resulting in almost undetectable levels of non-specific adsorption (see numbers in Fig. 3A). The final injection of goat IgG (1 mg/ml) gave slightly higher adsorption levels, but the extent of ≤25 RU corresponds to less that 1% of a dense IgG monolayer (compare Fig. 1D) and still falls into the category of exceptionally low non-specific adsorption [Ostuni et al., 2001].

Non-specific adsorption of DNA was also tested and found to be insignificant (Fig. S13). At the same time, a biotinylated oligonucleotide (a 30-mer) was seen to bind on top of streptavidin with high efficiency (420 RU) and to hybridize with the complementary single-stranded DNA (see Fig. S13).

3.5. Stability of the biotin-streptavidin-biotin bridge during prey removal

Conventionally, bait molecules are immobilized on the chip surface by covalent coupling [Cooper, 2009]. In this context, the term "chip regeneration" means that all bound prey molecules are removed from the chip, making it ready for the next injection of a prey-containing sample (see Scheme 1A). Typical methods for prey removal make use of short pulses of HCl (1-100 mM), glycine buffer (pH 1.7-2.5), NaOH (6-100 mM), SDS, or denaturants, as reviewed recently [Goode et al., 2015].

Although our new chips allow for "full regeneration" of the protein-free desthiobiotin surface (Scheme 1A), it is very important that we also have the option of performing many cycles of prey binding and prey removal (see Scheme 1A). The characterization of a biospecific interaction requires many injections of the same prey at different concentrations during all of which the biotinylated bait should remain firmly immobilized on the streptavidin surface (see Figs. 4 and 5). On a conventional chip with covalently bound baits, pulses of acid or base or SDS can only cause denaturation of the bait but the bait cannot get lost. On our desthiobiotin chips, however, streptavidin and the biotinylated bait are bound via non-covalent bonds, therefore it was essential to find out whether these persist while using common methods of prey removal.

Here we tested the stability of streptavidin-bound biotin-IgG during applications of 15 s pulses of HCl (Fig. 3B), sodium carbonate (Fig. S14), NaOH (Fig. S15), and glycine buffer (pH 2.5, Figs. 4-5 and S16-S17). The different HCl (or NaOH) concentrations were prepared

by mixing 100 mM HCl (or 100 mM NaOH) with 100 mM NaCl, so that the ionic strength remained uniform in spite of varying HCl (or NaOH) concentrations. The different sodium carbonate buffers were prepared by adjusting a 100 mM Na_2CO_3 solution to pH 11.0, 10.5, or 10.0 with concentrated HCl.

The double layer of streptavidin and biotin-IgG was resistant to 10-100 mM HCl (Fig. 3B, blue solid trace), while the single layer of streptavidin was only fully stable at 10 mM HCl (red dashed trace). These findings leave us with two options for prey removal by HCl: (i) the use of 10 mM HCl, or (ii) the stabilization of the streptavidin layer in the control cell with an inert biotinylated protein (e.g., biotin-BSA), which enables us to use up to 100 mM HCl for bait removal.

Sodium carbonate buffers (pH 10-11) also proved to be well applicable for prey removal (Fig. S14). A minor unexpected response was the small *increase* in the resonance angle of the streptavidin monolayer, which was regularly seen after the first injection of basic buffer (red trace in Fig. S14). Nevertheless, sodium carbonate can readily be used for bait removal if a dummy injection with carbonate is applied before the first injection of the bait; if this is done, the baseline reaches a new stable value.

NaOH (10-100 mM) appears unsuitable for bait removal, since it causes a significant loss of the chip-bound streptavidin ± biotin-IgG (see Fig. S15). The unfavorable effect of 10 mM NaOH (pH 11) is obviously due to its low ionic strength, because 100 mM sodium carbonate (pH 11) caused no undesired bait removal (Fig. S14).

Perfect stability of the chip-bound bait was found when 1 M glycine (pH 2.5, for 3 min) was used for bait removal (Fig. S16). On the other hand, small losses were seen when 100 mM glycine (pH 2.5, for 3 min, Fig. S17) was employed. These observations confirm the hypothesis that high ionic strength protects chip-bound baits from being dissociated by the reagent that is used for prey removal. The same effect had consistently been found when avidin mutants were used for the immobilization of biotinylated baits on biotin-SAMs [Zauner et al., 2016].

It should be mentioned that 0.5% SDS can also be applied for the removal of the prey from streptavidin-bound bait so long as that prey is not denatured by SDS. We found this method to be applicable for the calmodulin-binding peptide; the removal of calmodulin by glycine (pH 2.5, Figs. 5A and S17) could also be performed with 0.5% SDS (data not shown).

In conclusion, the desthiobiotin-streptavidin-biotin bridge between the chip surface and the bait molecule is resistant to the reagents like HCl, Na_2CO_3, or SDS which are commonly used for in the sense of "prey removal" (see Scheme 1A). Hereby, an ionic strength of ≥200 mM was found to be advantageous. As a consequence, a chip with an immobilized biotinylated bait can be used in the same way as a chip with a covalently bound bait. Only when desired, the chip-bound streptavidin plus bait is removed by the "full regeneration" method that is illustrated in Scheme 1A and exemplified in Fig. 2.

3.6. Measurement of the interaction between protein G and human IgG2κ

The reversible binding of human IgG2κ to chip-bound biotin-protein G had previously been measured to test the performance of regenerative chips which relied on switchable avidin mutants [Pollheimer et al., 2013; Zauner et al., 2016]. In our study, the same test was applied to the new desthiobiotin chip where wild-type streptavidin was used for immobilization of biotinylated protein G.

The entire experiment is presented in Fig. S16. Both cells were functionalized with streptavidin, whereby biotin-BSA was immobilized in the control cell (see Fig. 4B) and biotin-protein G was bound in the sample cell (see Fig. 4A). After a dummy injection of 1 M

glycine (pH 2.5), many different concentrations of IgG2κ were injected; 1 M glycine (pH 2.5) was used for prey removal after each injection. The data were processed by the double referencing method [Rich and Myszka, 2000; Pollheimer et al., 2013], yielding the experimental bindings curves which are shown in both Figs. 4C and 4D as solid colored curves.

A perfect fit of the binding curves was obtained with the "bivalent analyte model" (dashed traces in Fig. 4C), which assumes two binding steps: pre-binding of one IgG2κ to one protein G molecule, followed by bivalent binding of IgG2κ to two adjacent protein G molecules on the streptavidin surface (see Fig. 4A). The kinetic and equilibrium constants obtained from the fit were quite similar to those previously obtained on chips covered with avidin mutants instead of streptavidin [Zauner et al., 2016]. As previously found on avidin surfaces, it was impossible to fit the binding curves with the simple Langmuir model, which assumes only 1:1 binding between soluble IgG2κ and streptavidin-bound protein G (dashed traces in Fig. 4D).

In conclusion, the test with immobilized protein G and soluble IgG2κ demonstrates that the streptavidin monolayer on the regenerative chip is well suited for the reconstitution of the interaction mechanism between native protein G of *streptococcus sp.* and IgG molecules. Since Protein G is also found at high density on the surface of the microorganism [Fahnestock et al., 1986], the binding mechanism described in Fig. 4 is likely to also occur *in vivo*.

3.7. Measurement of calmodulin-peptide interactions

Fig. 5 presents two alternative strategies for studying the specific interaction between calmodulin (CaM) and the CaM-binding segment of smooth muscle myosin light chain kinase (smMLCK). These two proteins are known to interact in a simple 1:1 fashion, with a K_d of ~1 nM [O'Neill and DeGrado, 1993].

In the first approach, the CaM-binding peptide was anchored to the streptavidin monolayer by a C-terminal biotin group (Fig. 5A), and soluble CaM was injected at different concentrations in presence of 2 mM Ca^{2+} (Fig. 5C). Interestingly, the immobilization of the peptide was much more efficient if maleimide-PEG_{11}-biotin was first bound to streptavidin and the peptide was then covalently coupled to the maleimide group (see Chart S5 and Fig. S17). This is very fortunate, because *in situ*-coupling of a thiol-peptide (or of thiol-DNA) is much faster and easier than biotinylation in solution and purification of the biotinylated peptide by reversed phase chromatography. The complete SPR experiment (with the coupling step) is shown in Fig. S17. The resulting binding curves (solid traces in Fig. 5C) could readily be fitted to a simple 1:1 binding model (dashed traces in Fig. 5C) with a K_d value of 0.4 nM.

In the complementary approach (Fig. 5B), CaM was first labeled with biotin, purified by gel filtration, immobilized on the streptavidin surface, and then probed with different concentrations of nearly the same smMLCK peptide (it lacked only the C-terminal cysteine). The corresponding binding curves (solid traces in Fig. 5D) could also be fitted to the simple 1:1 binding model (dashed traces in Fig. 5D), yielding the same K_d value (0.4 nM) as with the immobilized peptide in Fig. 5C.

3.8. Quantification of antigens in crude biofluids

Above, the new regenerative chip was shown to be very useful for biological interaction analysis with purified components. In parallel it was interesting to find out whether the new chip can be used for quantification of analyte molecules in crude biofluids, preferably by the standard addition technique.

For comparison we chose a study where a monoclonal anti-His_6 tag antibody had been covalently coupled to a CM5 chip at an immobilization level of >13600 RU and a linear dose-

response (from 45 to 1850 RU) of GFP-His_6 binding had been reported between 3 and 170 nM antigen concentration, as needed for standard addition [Ekström, 2012].

In our experiments (section S13 in the Supplementary Information) we used His_6-tagged enhanced GFP (His_6-GFP) as the analyte and a biotinylated monoclonal anti-GFP antibody as the bait molecule. As expected for our two-dimensional surface, the immobilization level of the biotinylated antibody was much lower (2508 RU, Fig. S20) than that on the CM5 chip. Accordingly, the linear regime of the dose-response to the antigen was less pronounced (from 3 to ~25 nM) and the responses for these concentrations of antigen were much smaller (from 6 to 48 RU, Fig. S22). When potential matrix effects on the dose response were ignored, then the comparison of the calibration curve (Fig. S22) with the dose-response of crude lysate (Fig. S23) allowed for estimation of antigen concentration with an accuracy of ~20% (Fig. S24). Explicit determination of the matrix effect by the standard addition method was, however, precluded by the narrow range of the linear dose-response on our chip.

Overall the results with serum and bacterial lysate were much better than we had dared to expect. For the following reasons, we find them very encouraging: (i) On antibody-functionalized surfaces, the non-specific adsorption from crude biofluids was surprisingly low. (ii) The problem of low antibody immobilization levels and low dose-responses to antigen will become irrelevant when label-enhanced SPR is employed, since the signal-to-noise ratio is about 100-fold better there than in label-free SPR [Eng et al., 2016; Granqvist et al., 2013]. In addition, label-enhanced SPR amplifies only the specific response but not the non-specific responses. For these reasons, we think that it could be very well possible to exploit the potential of our regenerative chip surfaces not only for biological interaction analysis but also for quantification of analytes in crude biofluids.

4. Conclusions

The new desthiobiotin-SAM shows the same high protein resistance and binding capacity for streptavidin as previously found for the analogous biotin-SAM [Pollheimer et al., 2013]. In contrast to the latter, however, the new desthiobiotin-SAM can be re-used with different bait molecules as often as desired within a period of 2-3 weeks. Even tenaciously bound double layers consisting of streptavidin plus biotinylated proteins are completely removed by 3 min injections of biotin, GTC, pepsin, and SDS, without any negative impact on the chip performance.

Fortunately, streptavidin and the biotinylated bait can only be removed by the reagents named above, while no loss of biotinylated bait is observed with most of the reagents (HCl, Na_2CO_3, and SDS) that are commonly used for removal of prey molecules. This means that numerous cycles of prey binding and prey removal can be performed with one type of biotinylated bait.

Due to the fact that it makes it possible to strictly distinguish between mere prey removal on the one hand, and rigorous removal of streptavidin along with the bait on the other hand, the new desthiobiotin chip appears to be ideal for the rapid testing of numerous bait-prey interactions. Its costs are very low, and it can be employed in a fully automated manner.

Acknowledgements

This work was supported by the government of Upper Austria (project DK Nanocell). We are grateful to one of the reviewers for the suggestion that we try to quantify proteins in crude biofluids and to Theresa Zacherl and Theresa Schwarz for overexpression of His_6-GFP.

Appendix A. Supplementary information

Supplementary material associated with this article can be found in the online version at http://…

References

Cooper, M.A., 2009. Sensor surfaces and receptor deposition, in: Cooper, M.A. (Ed.), Label-free biosensors. 1st ed. Cambridge, New York, Melbourne, Madrid, Cape Town, Singapore, Sao Paolo, Delhi: Cambridge University Press, pp. 110-142.

Ekström, E. 2012. SPR-based method for concentration determination of proteins in a complex environment. Thesis at Uppsala University School of Engineering. 37 pages.

Eng, L., Nygren-Babol, L., Hanning, A. 2016. Anal. Biochem. 516, 79-87.

Fahnestock, S.R., Alexander, P., Nagle, J., Filpula, D., 1986. J. Bacteriol. 167, 870-880.

Goode, J.A., Rushworth, J.V.H., Millner, P.A. 2015. Langmuir 31, 6267-6276.

Granqvist, N., Hanning, A., Eng, L., Tuppurainen, J., Viitala, T. 2013. Sensors 13, 15348-15363.

Green, N.M. 1990. Methods Enzymol. 184, 51-67.

Gruber, H.J., 2017. PCT Application "Regenerative Biosensor". Published on February 23, 2017 under the number WO/2017/029194 A1.

Hirsch, J.D., Eslamizar, L., Filanoski, B.J., Malekzadeh, N., Haugland, R.P., Beechem, J.M., Haugland, R.P., 2002. Anal. Biochem. 308, 343-357.

Jung, L.S., Nelson, K.E., Stayton, P.S., Campbell, C.T., 2000. Langmuir 16, 9421-9432.

Knoll, W., Zizlsperger, M., Liebermann, T., Arnold, S., Badia, A., Liley, M., Piscevic, D., Schmitt, F.-J., Spinke, J. 2000. Coll. Surf., A 161, 115-137.

Matsumoto, E., Fukuda, T., Miura, Y. 2011. Coll. Surf. B: Biointerfaces 94, 280-284.

O'Neil, K.T., DeGrado, W.F. 1993. Trends Biochem. Sci. 15, 59-64.

Ostuni, E., Chapman, R.G., Holmlin, R.E., Takayama, S., Whitesides, G.M., 2001. Langmuir 17, 5605-5620.

Pollheimer, P., Taskinen, B., Scherfler, A., Gusenkov, S., Creus, M., Wiesauer, P., Zauner, D., Schöfberger, W., Schwarzinger, C., Ebner, A., Tampé, R., Stutz, H., Hytönen, V.P., Gruber, H.J., 2013. Bioconjugate Chem. 24, 1656-1668.

Porath, J., Maisano, F., Belev, M. 1985. FEBS Lett. 185, 306-310.

Prime, K.L., Whitesides, G.M., 1991. Science 262, 1164-1167.

Raphael, M.P., Rappole, C.A., Kurihara, L.K., Christodoulides, J.A., Qadri, S.N., Byers, J.M. 2011. J. Fluoresc. 21, 647-652.

Rich, R. L., Myszka, D.G., 2000. Curr. Opin. Biotechnol. 11, 54-61.

Taskinen, B., Zauner, D., Lehtonen, S.I., Koskinen, M., Thomson, C., Kähkönen, N., Kukkurainen, S., Määttä, J.A.E., Ihalainen, T.O., Kulomaa, M.S., Gruber, H.J., Hytönen, V.P., 2014. Bioconjugate Chem. 25, 2233-2243.

Yoon, H.C., Hong, M.-Y., Kim, H.-S. 2001. Langmuir 17, 1234-1239.

Zauner, D., Taskinen, B., Eichinger, D., Flattinger, C., Ruttmann, B., Knoglinger, C., Traxler, L., Ebner, A., Gruber, H.J, Hytönen, V.P. 2016. Sens. Actuators B: Chem. 229, 646-654.

Fig. 1. Reversible immobilization of streptavidin (± biotinylated protein) on mixed self-assembled monolayers (SAMs) with desthiobiotin groups. (A) SAM with 10% desthiobiotin component **2** [Knoll et al., 2000]. (B) SAM with 20% desthiobiotin component **4** (this study). (C) Repeated immobilization of wild-type streptavidin on the mixed SAM shown in panel B, using guanidinium thiocyanate (GTC, 6M). (D) Repeated immobilization of streptavidin ± biotin-IgG on the mixed SAM in panel B, using GTC (with 4 mM TCEP), pepsin (2 mg/ml, in 1 M glycine, pH 2.5), and SDS (0.5%).

Fig. 2. Optimized protocol for removal of streptavidin plus biotinylated bait from a mixed desthiobiotin SAM. Pepsin was dissolved in 1 M glycine (pH 2.5). Data reproduced from Gruber [2017] with permission.

Fig. 3: Critical properties of the new regenerative sensor chip. (A) Absence of non-specific protein adsorption was tested by sequential injections of lysozyme (in FC2), BSA (2× in FC2), and IgG (in both flow cells). (B) Resistance of bound streptavidin (± biotin-IgG) to injection of different HCl concentrations. The sum of [HCl] + [NaCl] was always 100 mM. Pepsin was dissolved in 100 M glycine (pH 2.5). Data in panel A reproduced from Gruber [2017] with permission.

Fig. 4. Analysis of the interaction between immobilized biotin-protein G and soluble human IgG2κ. (A, B) Schematic depiction of the sensing layers in FC1 and FC2, respectively. The original SPR data set (Fig. S16) was processed by "double referencing" [Rich & Myszka, 2000; Pollheimer et al., 2013], in order to calculate the experimental binding curves (solid colored lines in panels C and D). (C) Global fit of the experimental binding curves with the bivalent analyte model (dashed lines). The data in panel C are reproduced from Gruber [2017] with permission. (D) Global fit of the same binding curves as in panel C with the simple 1:1 binding model (Langmuir model, dashed lines).

Fig. 5. Analysis of the interaction between calmodulin and the calmodulin-binding segment from smMLCK. (A) Interaction scheme for soluble calmodulin (shown in blue, with four bound Ca^{2+} ions) with immobilized peptide (shown in red). (B) Interaction scheme for soluble peptide (red) with immobilized biotin-calmodulin (bue). (C) Binding curves for soluble calmodulin, measured as illustrated in panel A and described in Fig. S17. (D) Binding curves for soluble smMLCK peptide, measured as illustrated in panel B and described in the Supplementary information (section S3, see "biotin-calmodulin"). The dashed lines in panels C and D are global fits with the simple Langmuir model, whereby mass transport limitations are taken into account. Doing so was justified, because the binding kinetics was dependent on the flow.

Scheme 1. Illustration of the reversible immobilization of biotinylated bait molecules on desthiobiotin surfaces. (A) Distinction between conventional regeneration ("prey removal") and full regeneration of the sensor chip (removal of streptavidin along with the biotinylated bait). Wild-type streptavidin remains tetrameric (5a), in contrast to switchable avidin mutants (5b) [Zauner et al., 2016]. (B) Removal of statistically biotinylated proteins requires guanidinium thiocyanate (GTC) plus pepsin. (C) Mono-biotinylated protein can be removed with GTC alone.

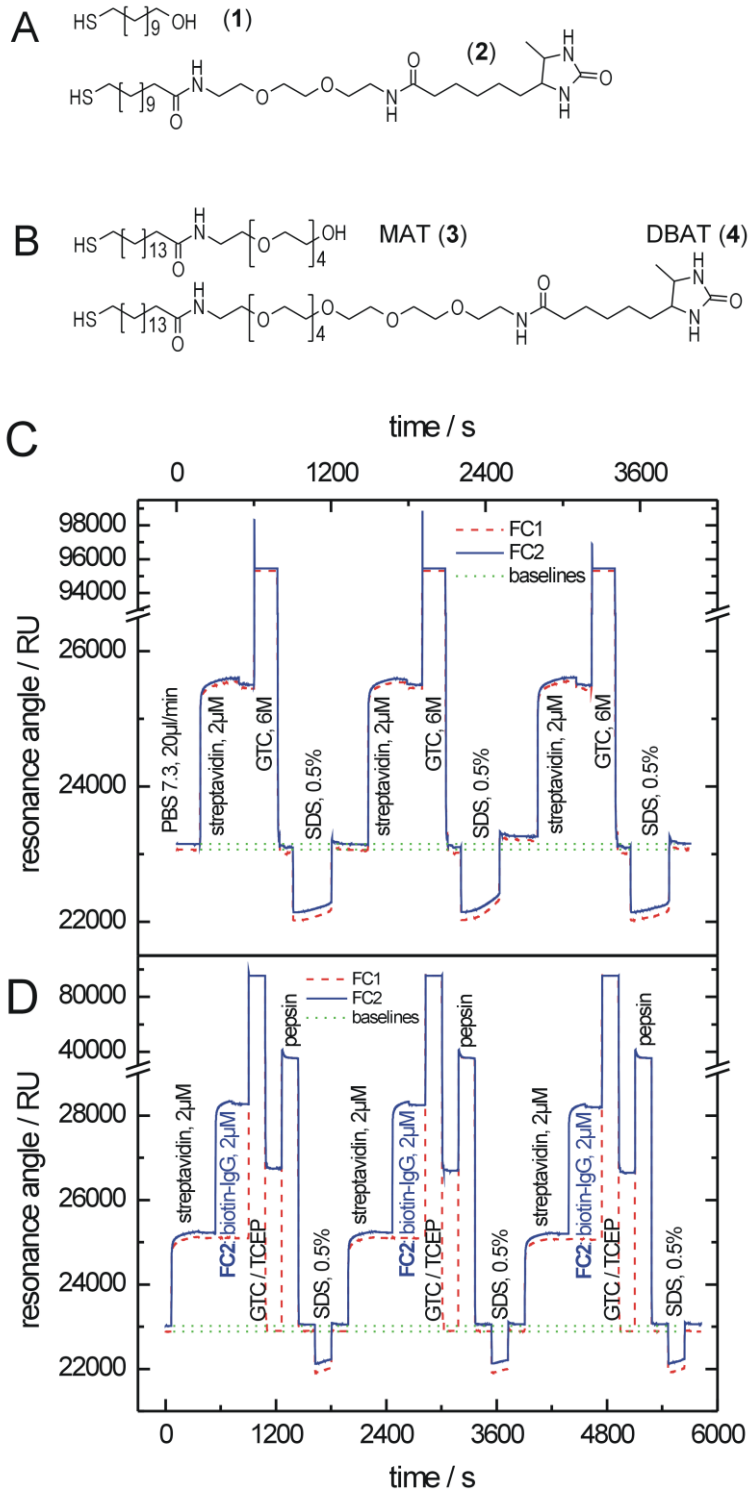

Fig. 1

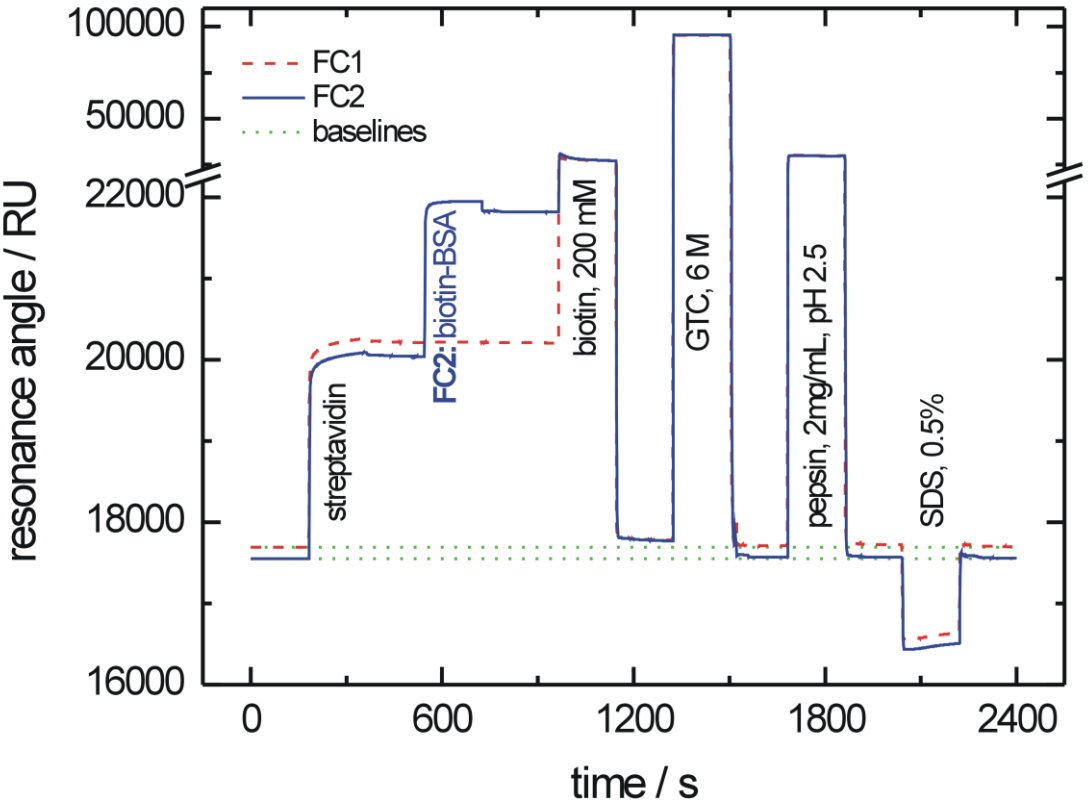

Fig. 2

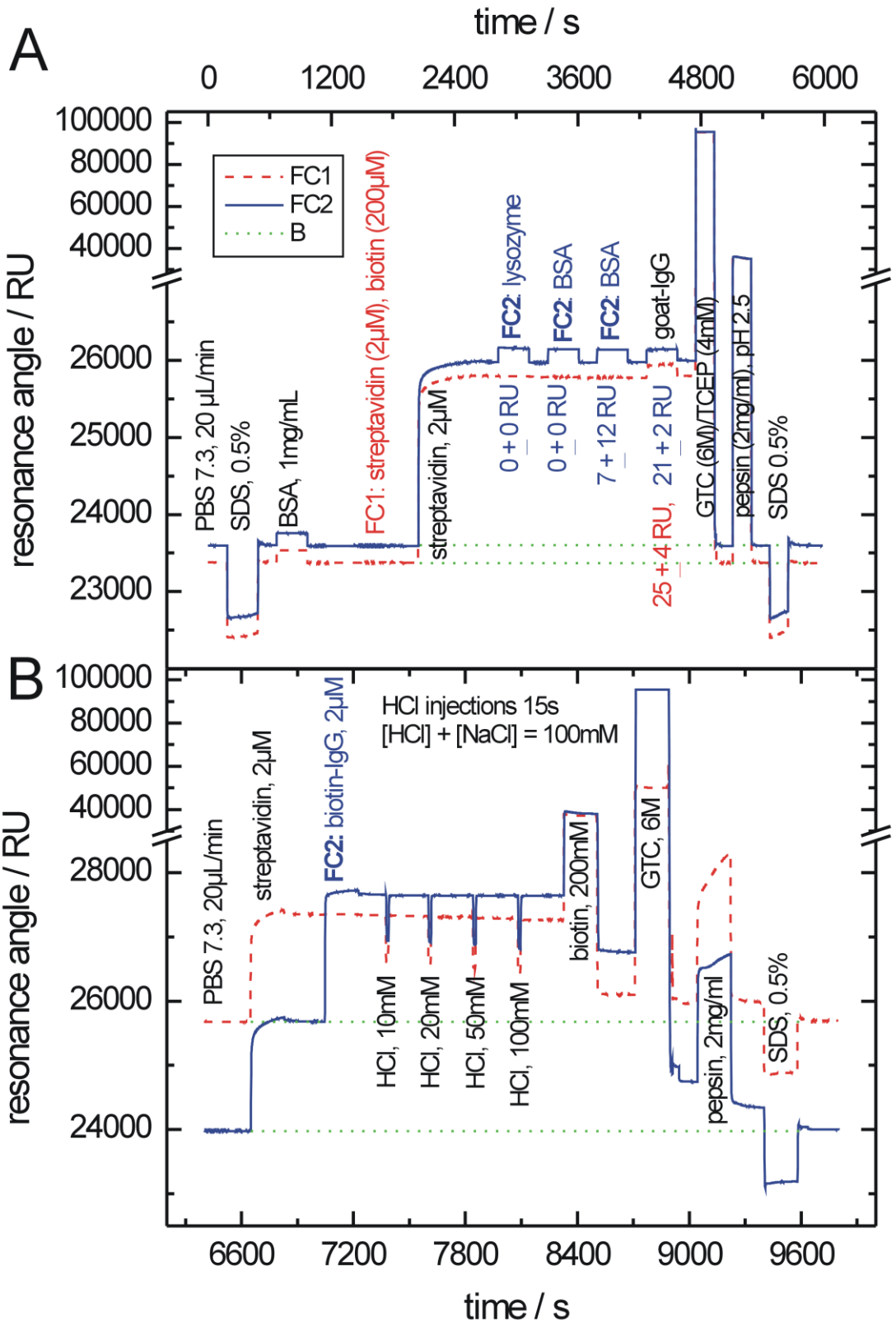
A
time / s
0
1200
2400
3600
4800
6000
100000
80000
60000
40000
26000
25000
24000
23000
resonance angle / RU
FC1
FC2
B
PBS 7.3, 20 µL/min
SDS, 0.5%
BSA, 1mg/mL
FC1: streptavidin (2µM), biotin (200µM)
streptavidin, 2µM
FC2: lysozyme
0 + 0 RU
FC2: BSA
0 + 0 RU
FC2: BSA
7 + 12 RU
goat-IgG
25 + 4 RU, 21 + 2 RU
GTC (6M)/TCEP (4mM)
pepsin (2mg/ml), pH 2.5
SDS 0.5%
B
100000
80000
60000
40000
28000
26000
24000
resonance angle / RU
PBS 7.3, 20µL/min
streptavidin, 2µM
FC2: biotin-IgG, 2µM
HCl injections 15s
[HCl] + [NaCl] = 100mM
HCl, 10mM
HCl, 20mM
HCl, 50mM
HCl, 100mM
biotin, 200mM
GTC, 6M
pepsin, 2mg/ml
SDS, 0.5%
6600
7200
7800
8400
9000
9600
time / s

Fig. 3

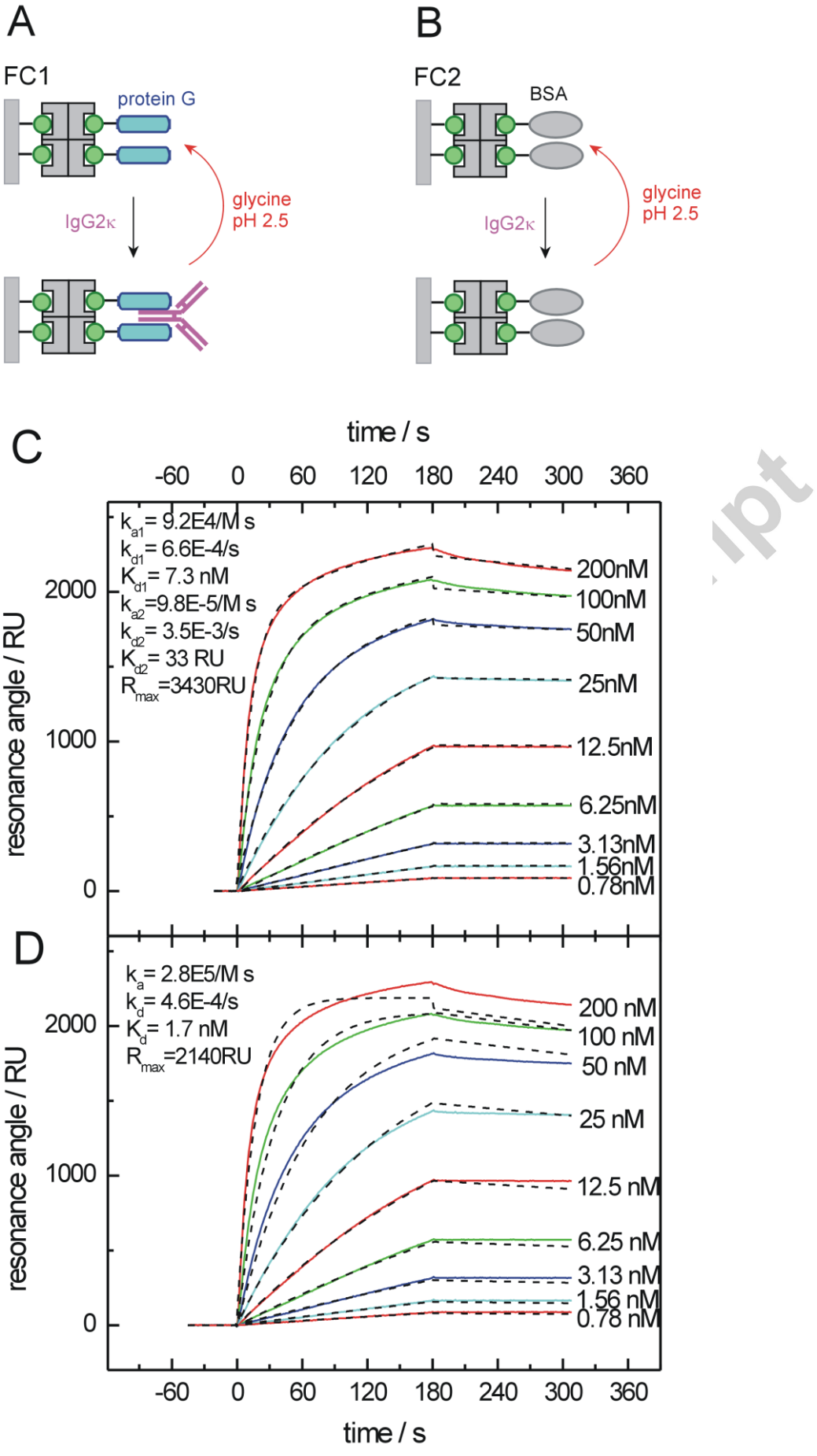
A
FC1
protein G
IgG2κ
glycine
pH 2.5
B
FC2
BSA
IgG2κ
glycine
pH 2.5
C
time / s
-60 0 60 120 180 240 300 360
k_{a1}= 9.2E4/M s
k_{d1}= 6.6E-4/s
K_{d1}= 7.3 nM
k_{a2}=9.8E-5/M s
k_{d2}= 3.5E-3/s
K_{d2}= 33 RU
R_{max}=3430RU
200nM
100nM
50nM
25nM
12.5nM
6.25nM
3.13nM
1.56nM
0.78nM
resonance angle / RU
2000
1000
0
D
k_a= 2.8E5/M s
k_d= 4.6E-4/s
K_d= 1.7 nM
R_{max}=2140RU
200 nM
100 nM
50 nM
25 nM
12.5 nM
6.25 nM
3.13 nM
1.56 nM
0.78 nM
resonance angle / RU
2000
1000
0
-60 0 60 120 180 240 300 360
time / s

Fig. 4

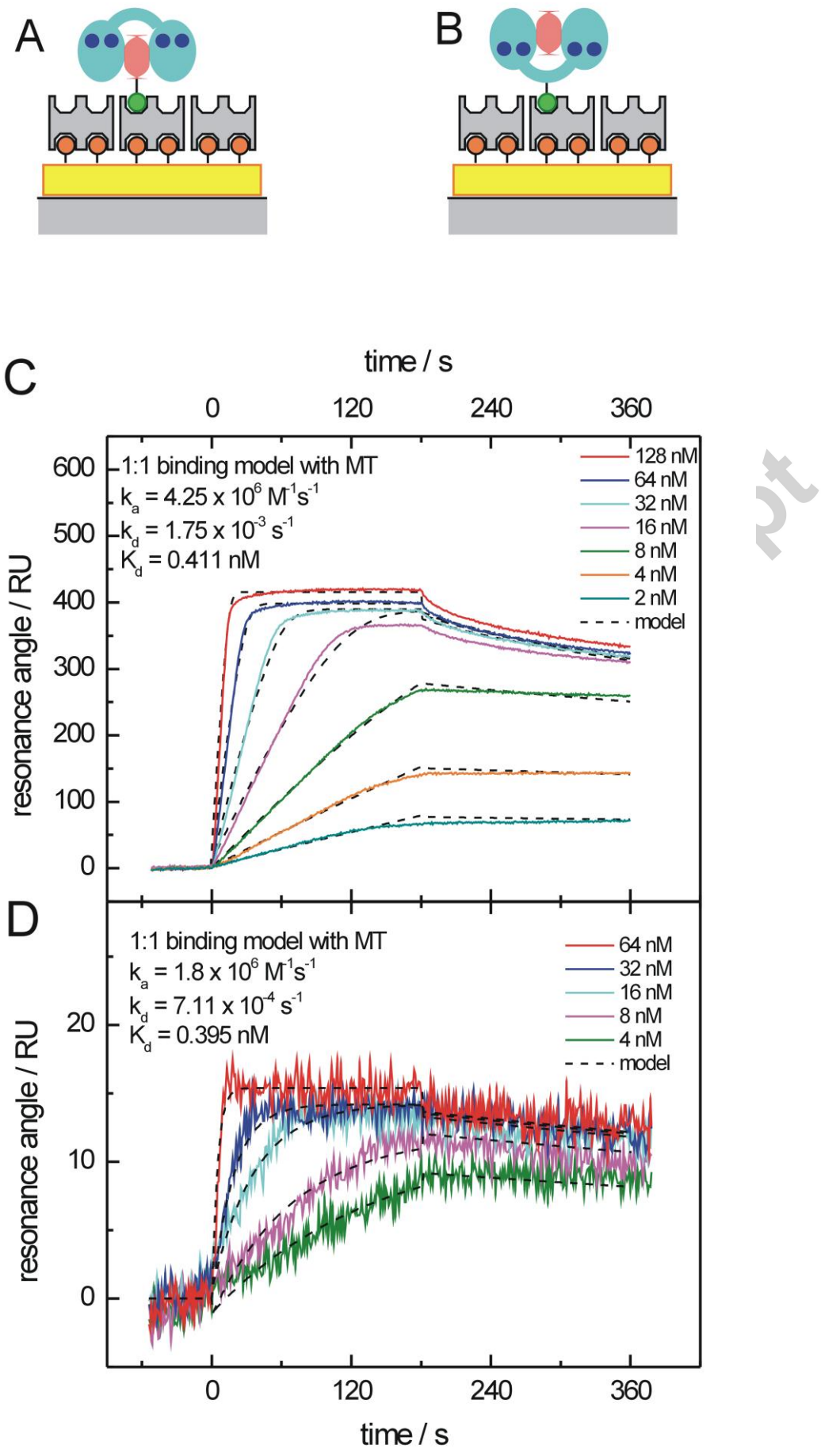
A
B
C
time / s
0
120
240
360
600
500
400
300
200
100
0
resonance angle / RU
1:1 binding model with MT
k_a = 4.25 x 10^6 $M^{-1}s^{-1}$
k_d = 1.75 x 10^{-3} s^{-1}
K_d = 0.411 nM
128 nM
64 nM
32 nM
16 nM
8 nM
4 nM
2 nM
model
D
1:1 binding model with MT
k_a = 1.8 x 10^6 $M^{-1}s^{-1}$
k_d = 7.11 x 10^{-4} s^{-1}
K_d = 0.395 nM
64 nM
32 nM
16 nM
8 nM
4 nM
model
20
10
0
resonance angle / RU
0
120
240
360
time / s

Fig. 5

Graphical Abstract

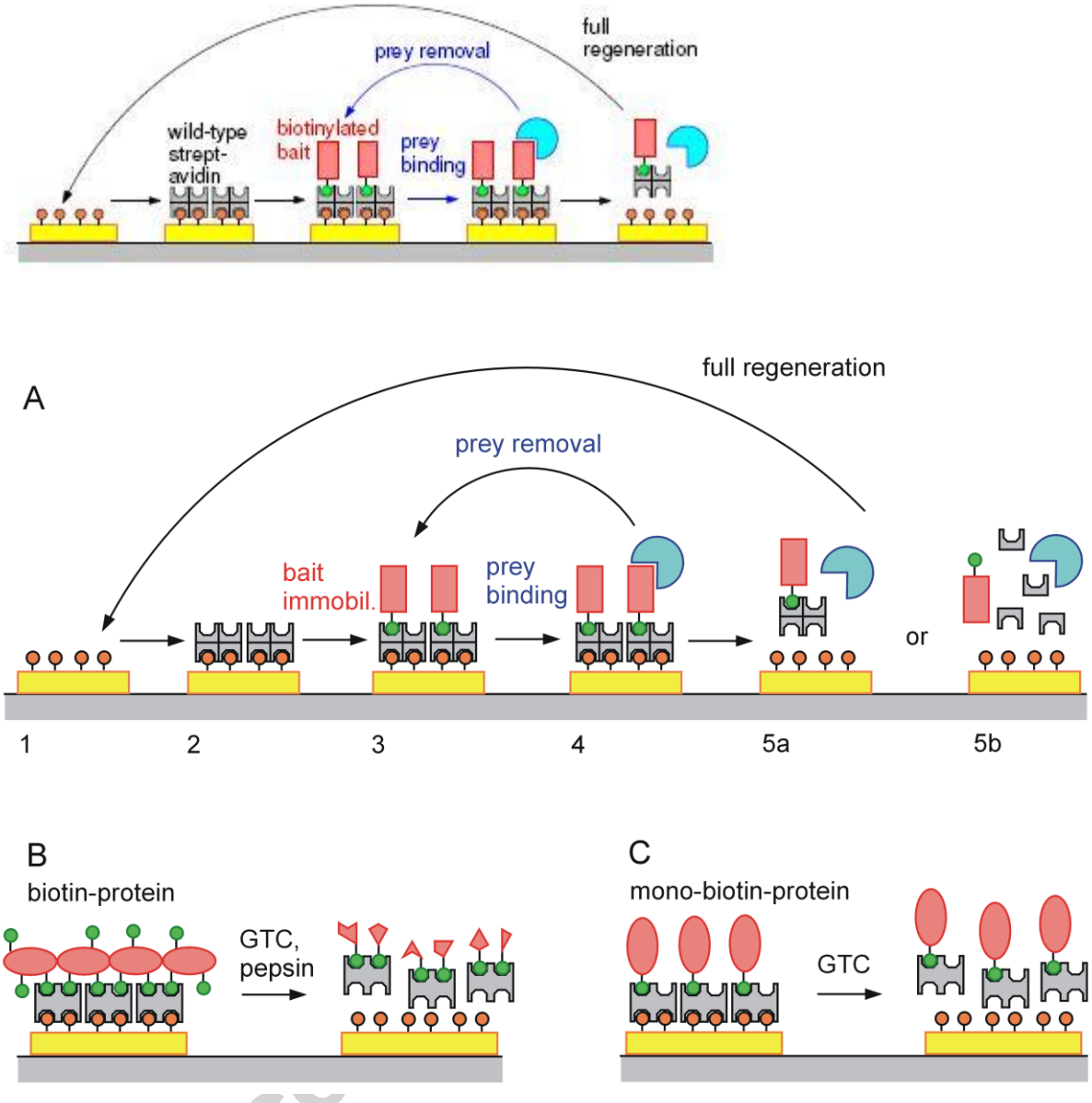

Scheme